

Dynamical Mode Recognition of Coupled Flame Oscillators by Supervised and Unsupervised Learning Approaches

Weiming Xu^{a,#}, Tao Yang^{b,#}, and Peng Zhang^{a,*}

a Department of Mechanical Engineering, City University of Hong Kong, Kowloon Tong, Kowloon, 999077, Hong Kong

b Department of Mechanical Engineering, The Hong Kong Polytechnic University, Hung Hong, Kowloon, 999077, Hong Kong

Abstract

Combustion instability in gas turbines and rocket engines, as one of the most challenging problems in combustion research, arises from the complex interactions among flames, which are also influenced by chemical reactions, heat and mass transfer, and acoustics. Identifying and understanding combustion instability is essential to ensure the safe and reliable operation of many combustion systems, where exploring and classifying the dynamical behaviors of complex flame systems is a core task. To facilitate fundamental studies, the present work concerns dynamical mode recognition of coupled flame oscillators made of flickering buoyant diffusion flames, which have gained increasing attention in recent years but are not sufficiently understood. The time series data of flame oscillators are generated by fully validated reacting flow simulations. Due to limitations of expertise-based models, a data-driven approach is adopted. In this study, a nonlinear dimensional reduction model of variational autoencoder (VAE) is used to project the simulation data onto a 2-dimensional latent space. Based on the phase trajectories in latent space, both supervised and unsupervised classifiers are proposed for datasets with well known labeling and without, respectively. For labeled datasets, we establish the Wasserstein-distance-based classifier (WDC) for mode recognition; for unlabeled datasets, we develop a novel unsupervised classifier (GMM-DTWC) combining dynamic time warping (DTW) and Gaussian mixture model (GMM). Through comparing with conventional approaches for dimensionality reduction and classification, the proposed supervised and unsupervised VAE-based approaches exhibit a prominent performance for distinguishing dynamical modes, implying their potential extension to dynamical mode recognition of complex combustion problems.

Keywords: Variational autoencoder; Dynamical mode recognition; Coupled flames; Wasserstein distance; Dynamic time warping

* Corresponding author

E-mail address: penzhang@cityu.edu.hk, Tel: (852)34429561.

The authors equally contributed to the work.

1. Introduction

Diffusion flames are ubiquitous in nature (e.g. wildland and urban fires), domestic applications (e.g. fireplaces and furnaces), and industrial applications (e.g. gas-turbine and rocket engines). In a diffusion flame, the fuel and oxidizer are initially and spatially separated, and so it is often referred to as a non-premixed flame. These combustion phenomena involve complex processes of fluid mechanics, chemical reaction kinetics, thermodynamics, etc., where outputs are influenced by factors such as the composition and properties of the fuel, the availability of the oxidizing agent (usually oxygen), and the reaction conditions (for example, temperature and pressure). Understanding and controlling these factors is crucial for optimizing combustion processes and minimizing environmental impacts. Previously, the control and monitoring of combustion instabilities have been achieved through combustion system designing and modeling[1]. However, as the complexity of combustion systems increases, the difficulty of building the combustion models increases dramatically.

Flickering flame, as a classical unsteady flame configuration, was experimentally observed as the vibratory motion of Bunsen diffusion flames (referred to as “the flicker of luminous flames”) by Chamberlin and Rose[2]. They found that “the upper portion of the luminous zone rises to a maximum height ten times per second”, and that “this rate of vibration is not greatly affected by change in conditions”. Such a flame vibration was also observed in pool fires (called puffing fire[3]) and premixed flames[4, 5]. In recent years, coupled flickering diffusion flames have increasingly gained attention, as larger systems of flickering buoyant diffusion flames give rise to richer dynamical phenomena. Kitahata et al.[6] reported that two identical oscillating candle flames exhibit in-phase and anti-phase modes by increasing the distance between the flames. Okamoto et al.[7] observed four distinct dynamical modes of three flickering candle flames in an equilateral triangle arrangement, such as the in-phase, partial in-phase, rotation, and death modes. Manoj et al.[8] experimentally found variants of clustering and chimera states of more than 5-7 candle-flame oscillators in annular networks.

However, conventional knowledge-based approaches for mode recognition of coupled flickering flames have faced challenges, particularly when the complexity of a flame system increases. Challenges arise with phenomena such as large flame groups, which pose obstacles in feature extraction through expert knowledge, as well as high turbulent flow and intense interactions between chemistry and flow. Therefore, the present study aims to develop deep learning-based methods for dynamical mode recognition of coupled flame oscillators made of identical flickering flames.

The first challenge of the study is to deal with the intrinsically infinite dimension of flames, which are described by a set of partial differential equations accounting for the conservation laws. To enable latent features within the lower dimensional space, the primary approach involves identifying an effective low-dimensional latent representation of high-dimensional dynamical data[9-11]. Many linear reduction techniques, such as principal component analysis (PCA)[12] and proper orthogonal decomposition (POD)[13], have been utilized in extensive applications. However, the linear nature of these approaches may lead to suboptimal dimensionality reduction as the complexity of the nonlinear system increases [14]. Recently, deep learning (DL) has emerged as a prominent tool and has been found for various combustion issues[15], for example, data analysis, mode recognition, and physical modeling. Nonlinear dimensionality reduction methods have gained significant interest and have been gradually used in combustion applications. Arai et al.[16] used a variational autoencoder (VAE) to carry out the nonlinear reduction of various physics quantities in combustion systems. Iemura et al.[17] combined VAE and POD to analyze the flame oscillation phenomenon in the low-dimensional space. Considering the hidden states of complex combustion through time, Xu et al.[18] proposed a two-layer bidirectional long short-

term memory variational autoencoder (Bi-LSTM-VAE) model for dynamical mode recognition of multiple flame systems. By classifying the low-dimensional trajectories of different dynamical processes, combustion states can be distinguished and recognized.

In general, based on the adequacy of labeling in the dataset, mode recognition methods are categorized into supervised, semi-supervised, and unsupervised types. The first two methods play an important role in analyzing sufficient labeled data. Liu et al.[19] employed the multi-classified support vector machine (SVM) algorithm for supervised automatic classification of various combustion modes. Wang et al.[20] has introduced a supervised deep learning approach based on convolutional neural networks (CNN) and deep neural networks (DNN) for monitoring combustion status and predicting heat release rates. In those studies, ample data labels are crucial for achieving optimal performance, especially in the cases of supervised methods. In practice, datasets with labels are rare and the obtaining process is costly and poses significant challenges. Therefore, unsupervised clustering methods are extensively employed for complex combustion issues[15]. Among them, time series clustering is a type of data analysis technique for revealing the inherent structure and patterns in time-dependent data. Many previous studies found that time series clustering is highly effective for datasets with strong spatial-temporal characteristics. In fluid mechanics, Liu et al.[21] calculated the clustering index of wind turbines within a wind farm based on dynamic time warping (DTW) and implemented adaptive and unsupervised turbine clustering using the Gaussian mixture model (GMM). Barwey et al.[22] proposed a temporal axis clustering approach to enable mode recognition of similar regions of unsteady flow. In combustion, Mishra et al.[23] developed a novel hybrid unsupervised cluster-wise regression approach to represent the flamelet tables and speed up the computations in turbulent combustion simulations. Castellanos et al.[24] applied a k -means clustering algorithm to group combustion chemical features for constructing a lower order predictive model.

Despite the noteworthy studies in dimensional reduction and mode recognition, in discovering dynamical behaviors of coupled flickering diffusion flames, there are many interesting problems to be solved and the study is still in its infant stage. Consequently, the present was prompted by recognizing two key deficiencies in existing experimental studies and data analysis. Firstly, traditional methodologies struggle to recognize modes within high-dimensional complex systems due to the challenge of distilling features from expansive dynamical frameworks and discerning dynamic modes amidst the intricate interplay of physics and chemistry coupling. Secondly, a lack of robust and comprehensive frameworks for mode recognition persists, both in labeled and unlabeled datasets of coupled flickering flames.

In this study, the time series signals of the present coupled flickering flame system are the dataset, which can be extensively generated by numerical simulations. Both supervised and unsupervised mode recognition methods will be proposed for the presence or absence of known labeling in the dataset, respectively. First, this study will employ the nonlinear dimensionality reduction of VAE to obtain a two-dimensional phase trajectory of latent variables. Second, supervised and unsupervised classifiers will be utilized to analyze the lower dimensional phase trajectory. For the labeled dataset, the Wasserstein distance (WD) will be used to quantify distributional similarities of labeled and unlabeled phase trajectories for dynamic flame mode recognition. To deal with unlabeled time series, this study will combine a dynamic time warping (DTW) method and an unsupervised Gaussian mixture model (GMM) for effectively identifying the dynamic flame modes.

2. Deep Learning Methodology

Traditional methods encounter formidable challenges in mode recognition within high dimensional complex systems, grappling with the effective extraction of features from large-scale dynamical systems

and the discernment of dynamic modes amidst the intricate interactions between physics and chemistry coupling. Deep learning-based approaches have emerged as effective and alternative methodologies to address these challenges.

In this study, two supervised and unsupervised learning approaches for mode recognition of dynamically coupled flickering flames are developed based on the dimensionality reduction of VAE. The detailed structures of the designed VAE-WD and VAE-GMM-DTWC approaches are shown in Fig 1. The present datasets consist of m features and n samples from numerical simulations of flickering buoyant diffusion flames. Flame data are reconstructed through the four-layer encoder, two-dimensional latent representation, and four-layer decoder of VAE. For the phase trajectory of latent variables, the Wasserstein-distance-based supervised classifier and the GMM-DTW unsupervised classifier are employed to identify various dynamical modes of coupled flickering flames. The present approaches will be elaborated in the following subsections.

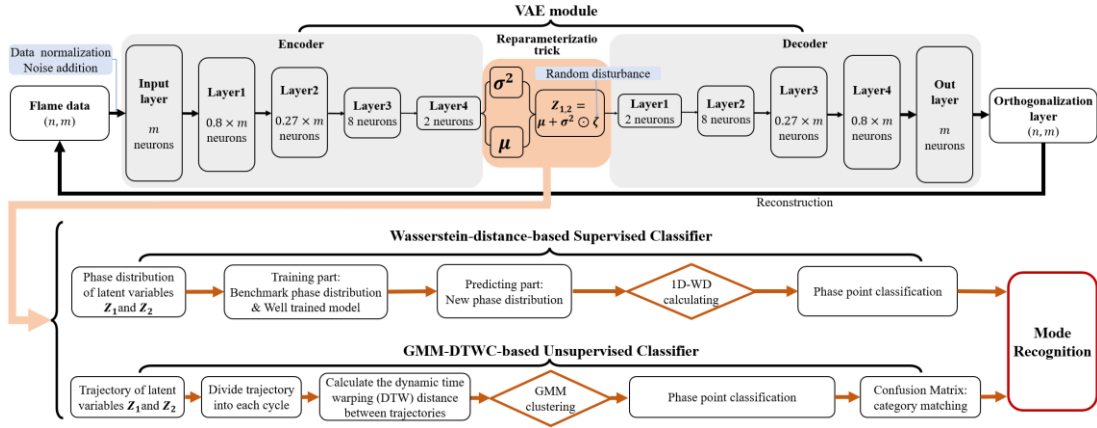


Fig 1. Structure of the designed VAE-Wasserstein-distance and VAE-GMM-DTWC approaches consisting of two modules: a neural network model of VAE and flowcharts of the supervised Wasserstein-distance-based classifier and the unsupervised GMM-DTW classifier.

2.1 Variational Autoencoder

Linear dimensional reduction models like PCA, POD, and DMD have been employed to extract dominant spatial-temporal features in combustion research. However, analyzing coupled flame oscillators poses a formidable challenge due to the intricate interplay of spatial-temporal coherent structures in high-dimensional nonlinear dynamics. Traditional linear methods struggle to address this complexity because their inherent linearity leads to performance degradation in nonlinear problems, requiring an excessive number of modes to achieve the same reconstruction accuracy as nonlinear dimensional reduction methods. Deep neural networks have emerged as an alternative to linear methods for their effectiveness in handling highly nonlinear problems. Hence, in this subsection, we describe a method for efficiently transforming high-dimensional trajectories into a simplified, low-order phase space. This is accomplished by employing a variational autoencoder, which holds great potential for application in various complex nonlinear systems.

Variational autoencoder (VAE), a powerful deep generative model, has been widely utilized to analyze the low-dimensional latent features of high-dimensional complex data. As shown in Fig.2, the nonlinear dimensionality reduction and reconstruction are carried out through the multiple neural network layers of the encoder and decoder modules. The time series of physical quantities in combustion systems are collected from multiple sensors distributed along each flame. The data collection will be

given in detail in Section 3. In the encoder component of the VAE, the feature vectors (m dimensions) are nonlinearly mapped by multiple neural network layers with decreasing numbers of neurons. The output of the four-layer encoder connects to a latent space (also called representation space) of two variables. In other words, those physical features can be encoded to a phase point of the latent space and the time series data can form a continuous phase trajectory in the two-dimensional phase plane. Then, the decoder component will reconstruct the physical features from the two latent variables through the multiple neural network layers with increasing numbers of neurons. Finally, an additional layer following the decoder is devised to orthogonalize the decoder output vector \mathbf{X}' into the orthogonal output vector \mathbf{X}'' . The objective is to minimize the mean square error between the reconstructed output and the original input. Simultaneously, a Kullback-Leibler (KL) divergence term is used to ensure that the phase distribution of latent variables aligns with a predefined prior distribution, namely the Gaussian distribution.

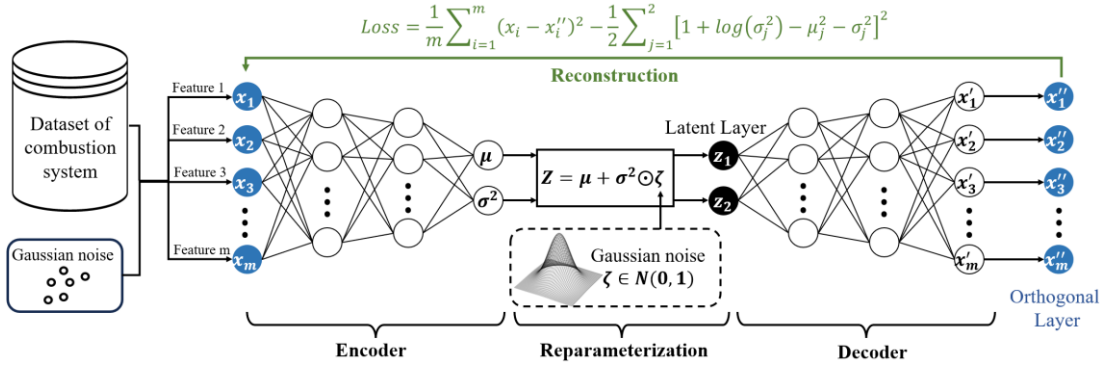


Fig 2. Data flow through the present VAE model: dataset, encoder, reparameterization, decoder, and orthogonal layer.

Specifically, the input $\mathbf{X} = \{x_1, x_2, \dots, x_n\}$ and the output $\mathbf{Y} = \{\mu, \sigma^2\}$ of the encoder is formulated as

$$\mathbf{Y} = f_E(\mathbf{W}_E \mathbf{X} + \mathbf{b}_E) \quad (1)$$

where \mathbf{W}_E and \mathbf{b}_E respectively correspond to the weights and bias matrixes of the encoder network, f_E is the activation function of the encoder, and all neural layers utilize the ReLU activation function. Particularly, the VAE incorporates a reparameterization trick to enhance gradient optimization. As illustrated in Eq. (2), the stochasticity is introduced into the latent variable $\mathbf{Z} = (z_1, z_2)$ through random sampling from a Gaussian noise $\boldsymbol{\varepsilon} \sim N(\mathbf{0}, \mathbf{I})$, thereby enabling the network to effectively optimize parameters. \odot denotes the Hadamard product.

$$\mathbf{Z} = \mu + \sigma^2 \odot \boldsymbol{\varepsilon} \quad (2)$$

In the decoder, \mathbf{Z} is reconstructed to $\mathbf{X}' = (x'_1, x'_2, x'_3, \dots, x'_n)$ with the same dimension of \mathbf{X} . The relationship between \mathbf{Z} and \mathbf{X}' is expressed as

$$\mathbf{X}' = f_D(\mathbf{W}_D \mathbf{Z} + \mathbf{b}_D) \quad (3)$$

where \mathbf{W}_D and \mathbf{b}_D respectively correspond to the weights and bias matrixes of the encoder network, f_D is the activation function of the decoder, utilizing the Sigmoid activation for the output layer, and the ReLU activation for all other layers. In addition, to enhance the better training dynamics and avoid issues like vanishing and exploding gradients from the reconstruction process, an orthogonal layer, initialized with orthogonal weight matrix, is employed to the encoder output \mathbf{X}' and produce \mathbf{X}'' :

$$X'' = W_{orthogonal}X' + b_{orthogonal} \quad (4)$$

$W_{orthogonal}$ indicates the weight of the last layer.

Algorithm 1: Train of the VAE

Model *encoder E and decoder D of the VAE.*

Input Data $X = \{x_1, x_2, \dots, x_n\}$ is split into X_{train}, X_{val} .

repeat:

for x **in** X_{train} : # x represents different batches of samples.

$\mu, \sigma \leftarrow f_E(W_E x + b_E)$

$z \leftarrow \mu + \sigma^2 \odot \varepsilon, \varepsilon \leftarrow N(0, I)$

$x' \leftarrow f_D(W_D z + b_D)$

$x'' \leftarrow W_{orthogonal}x' + b_{orthogonal}$

$Loss = Loss_{rec} + KL \leftarrow MSE(x, x''), -\frac{1}{2} \sum_{j=1}^2 (1 + \log(\sigma_j^2) - \mu_j^2 - \sigma_j^2)$

update $W_E, b_E, W_D, b_D, W_{orthogonal}, b_{orthogonal}$ using the backpropagation algorithm.

$Loss_{val} \leftarrow$ computed from X_{val}

if $Loss_{val} < \min(Loss_{val}.history)$ **then**

 save model, $\min(Loss_{val}.history) \leftarrow Loss_{val}$

else $count += 1$

if $count > stop_limit$ **then** stop training # $stop_limit$ is the stop setting of early stopping strategy.

until final epoch is reached

In the present VAE, the Adam optimization algorithm and the minibatch training method with a batch size of 64 are performed. Algorithm 1 represents the training process of the VAE. The model training process uses an early stopping strategy, either finishing 100 iterations with no loss reduction or reaching the pre-defined epoch limit of 2000. The reconstruction loss of present training and validation data in VAE is given in Fig. S1. The deep learning structure Pytorch is utilized as the backend computation library. Both the encoder and decoder components are respectively consisted of four layers, with $m, 0.8 \times m, 0.27 \times m, 8,$ and 2 neurons and $2, 8, 0.27 \times m, 0.8 \times m, m$ neurons, m denotes the number of collected features. All codes are run on the Google Colab platform, utilizing the platform's V100 GPU.

It's worth mentioning that the dimensionality reduction model in this paper serves the purpose of achieving precise dynamic pattern recognition. In our dataset, the two-dimensional latent space effectively captures reconstruction information, as demonstrated by the minimal reconstruction errors observed. Furthermore, the distribution of phase points for each mode within this two-dimensional latent space is distinct, suggesting a notable advantage in pattern recognition. These findings will be further elaborated upon in Section 4, emphasizing the robust representational power offered by a two-dimensional phase space for dynamic data.

2.2 VAE-WD classifier

Wasserstein distances (WD), inspired by the concept of optimal transportation, are metrics used to measure the similarity between probability distributions[25]. Widely applied in various mathematical fields such as fluid mechanics, partial differential equations, optimization, probability theory, and statistics, they hold significant theoretical importance. Moreover, they offer a successful framework for comparing diverse objects in practical applications like image retrieval, computer vision, pharmaceutical statistics, genomics, economics, and finance. Recent research by Chi et al.'s [26] has demonstrated the effectiveness of using the Wasserstein distance, a distance metric between probability distributions in phase space, for flame mode recognition. However, extracting features through expert knowledge may

encounter challenges as the complexity of a flame system increases, especially in the case of large flame groups, which can hinder feature extraction based on the brightness of individual flames.

To distinctly identify the various dynamic modes within the phase space of the nonlinear dimensionality reduction model VAE, it's crucial to ensure quantitative analysis of the mode recognition results. Inspired by this innovative approach and leveraging the capabilities of nonlinear reduced-order models (ROM), our study employs VAE to project high-dimensional flame data onto a non-overlapping phase space, bypassing the limitations of expert knowledge and adopting a data-driven approach. When dealing with a sufficiently labeled dataset, we utilize Wasserstein distance (WD) to evaluate the similarity among flame phase trajectories in Wasserstein distance space, enabling supervised mode recognition.

As shown in Fig. 3, the VAE-WD-based supervised classification has the training component for benchmark cases and the recognizing component for predicting cases. The first component is to train a VAE model and label the two-dimensional phase distribution of each known flame mode. The labeled phase trajectories are taken as benchmarks to classify different flame cases. The second component is to project a new set of flame data into the two-dimensional phase distribution via the well-trained VAE model and reshape the phase points into a one-dimensional sequence. The Wasserstein distance (aka the earth mover's distance [27]) is adopted to assess the similarity between the new distribution and each benchmark distribution. The one-dimensional sequence contains multiple circles. The average of WD values of all circles is calculated:

$$W(P, Q) = \frac{1}{N} \sum_{i=1}^N \inf_{\gamma \in \Gamma(p, q_i)} \int_{X \times Y} c(x, y) d\gamma(x, y) \quad (5)$$

where P and Q represent the one-dimensional sequence of the new and the benchmark, respectively. N denotes the number of circles of the benchmark. q_i is one of the circles of the benchmark distribution Q . $\Gamma(p, q_i)$ is the set of all joint distributions γ . X and Y are the spaces of the two distributions of p and q . $c(x, y)$ is the cost of transporting mass from x to y .

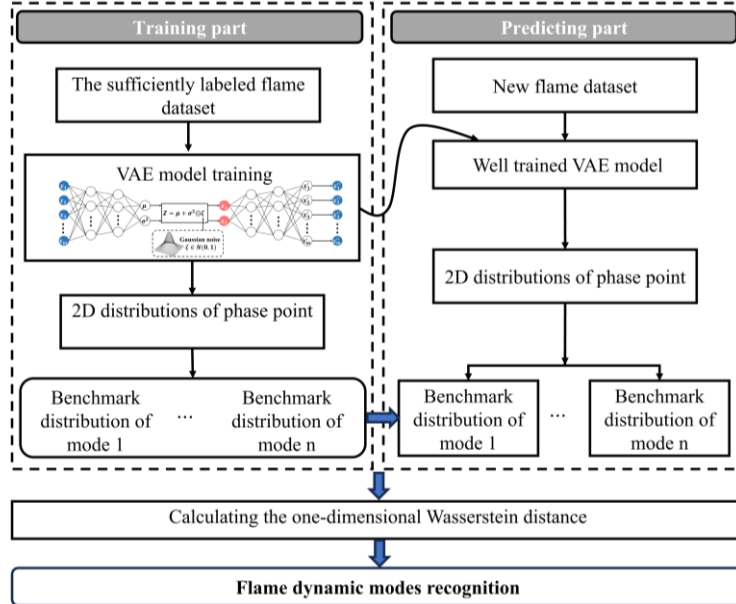


Fig 3. Structure of the VAE-WD classifier.

2.3 GMM-DTW classifier

Acquiring a thoroughly labeled dataset is often costly and challenging in industrial processes, particularly in complex combustion systems, where the scarcity of data and the complexity of structures

pose significant hurdles. Consequently, the development of effective unsupervised approaches for flame dynamic mode recognition emerges as a promising avenue. These methods provide valuable insights into the behaviors of dynamic modes in multi-flame systems, especially in scenarios where data is limited and not well-understood. Among these approaches, time series clustering stands out as an important method for uncovering the underlying structure and patterns in time-dependent data, particularly effective for analyzing datasets with strong spatial-temporal characteristics. Motivated by the work of Liu et al. [21], who applied the Dynamic Time Warping (DTW) algorithm to process time series data of active power between generators and achieved accurate clustering and classification using unsupervised methods. We utilize an unsupervised time series clustering method, leveraging the Gaussian Mixture Model (GMM) and DTW algorithm, to capture the temporal information of continuous physical phenomena observed in each cycle of the flame system, enabling accuracy mode recognition.

GMM, a type of machine-learning-based clustering method, has gained widespread popularity in mode recognition. GMM is a probabilistic model and consists of K sub-distributions, each of which is a single Gaussian distribution. The overall probability density function (PDF) of a GMM is formed by a weighted linear combination of individual Gaussian PDFs

$$P(X) = \sum_{i=1}^K \omega_i N(X|\mu_i, \Sigma_i) \quad (6)$$

$$N(X|\mu_i, \Sigma_i) = \frac{1}{\sqrt{2\pi|\Sigma_i|}} \exp\left\{-\frac{1}{2}(X - \mu_i)^T \Sigma_i^{-1} (X - \mu_i)\right\} \quad (7)$$

Where $N(X|\mu_i, \Sigma_i)$ is the probability distribution; $X = (x_1, x_2, \dots, x_n)$ is the input of GMM; ω_i ($\sum \omega_i = 1$), μ_i and Σ_i represent the weight, mean, and covariance matrix of the i -th Gaussian distribution, respectively.

Dynamic time warping (DTW), a type of time-series-based distance computation method, is utilized to compute the distance between two time series that have high similarity but do not perfectly sync up. For two time series of $Q = \{q_1, q_2, \dots, q_s\}$ and $C = \{c_1, c_2, \dots, c_t\}$, the $d(q_i, c_j)$ of a $s \times t$ distance matrix D is calculated

$$D[i, j] = d(q_i, c_j) = \sqrt{(q_j - c_j)^2} \quad (8)$$

where $D[i, j]$ represent the Euclidean distance between i -th component of the sequence Q and the c_j element in C . The warping path W is an $s \times t$ dynamic programming matrix with $W[i, j]$ for the alignment starts from $W[1, 1] = D[1, 1]$ and ends to $W[i, j]$. The path must satisfy constraints of boundedness, continuity, and monotonicity, and set all other elements in the first row and first column to infinity. DTW is the minimum accumulated distance by iterating the below equation

$$W[i, j] = D[i, j] + \min \{W[i - 1, j], W[i, j - 1], W[i - 1, j - 1]\} \quad (9)$$

where $W[i, j]$ is the accumulated distance from the start of the sequence $Q(q_1)$ to $Q(q_i)$ and from the start of the sequence $C(c_1)$ to $C(c_j)$. $W[i - 1, j]$, $W[i, j - 1]$, and $W[i - 1, j - 1]$ represent the path costs from the above, left, and diagonal grid points respectively. After computing the dynamic programming matrix W , we backtrack from the bottom-right grid point to find the optimal path, moving towards the top-left corner while selecting the path with the minimum cost at each step. This path represents the best match between the two sequences. By computing the total cost of this optimal path, we gauge the similarity between the sequences, with a smaller cost indicating a higher degree of similarity.

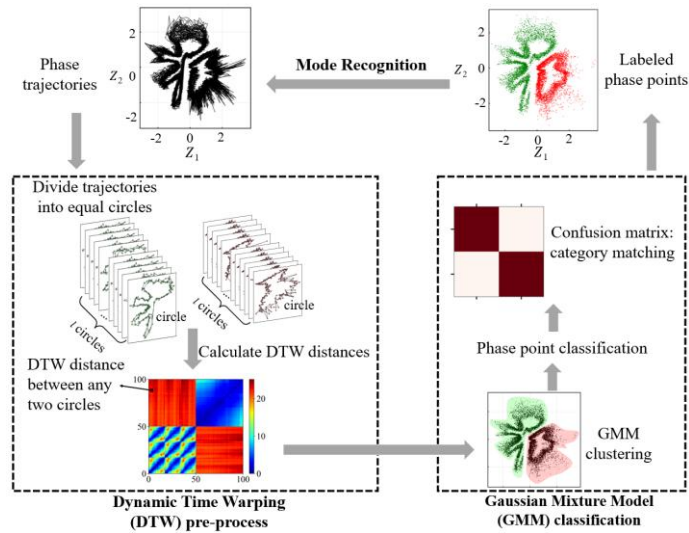


Fig 4. Data flow through the proposed unsupervised GMM-DTW classifier modules: DTW alignment distance calculation and GMM clustering.

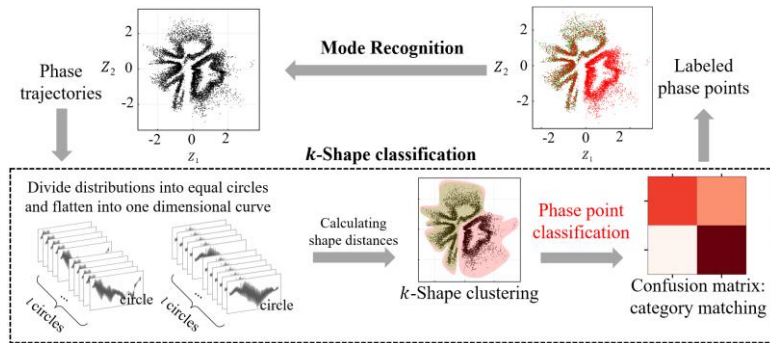


Fig 5. Data flow analysis of comparison unsupervised k-shape classifier module for time series: computing shape distances and cluster assignments.

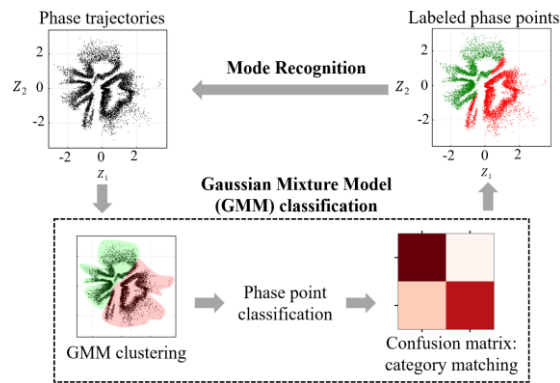


Fig 6. Data flow analysis of comparison unsupervised GMM classifier module for time series.

Dynamic Time Warping (DTW) has established itself as a cornerstone in various time series applications, including speech recognition, handwriting recognition, and activity recognition, owing to its adeptness in handling non-linear alignments. Building upon this foundation, we present a pioneering application of DTW in Dynamical Mode Recognition of Coupled Flame Oscillators. This groundbreaking approach signifies the first instance of utilizing DTW in flame mode recognition, a

domain characterized by highly nonlinear dynamics. By leveraging DTW's flexibility, we aim to precisely capture and compare the diverse dynamical modes exhibited by coupled flame oscillators, thereby advancing our understanding of these complex systems.

As shown in Fig. 4, this study incorporates the two approaches to effectively classify diverse dynamical modes of various coupled flickering flames. Specifically, this study employs the nonlinear reduced-order model VAE to map the high-dimensional flame data onto a two-dimensional latent space. Given the periodic nature of present dynamical flame systems, we capitalize on this characteristic by employing the DTW distance between any two cycles to extract features from the entire trajectory of the two latent variables. This approach ensures effectively capturing the continuous physical phenomena observed in each cycle of the flame system by measuring alignment distances between phase point trajectories. Particularly, the newly extracted features are clustered by GMM. This combination of DTW and GMM provides a robust framework for unsupervised mode recognition in coupled flickering flames. In addition, this study compared two other unsupervised classification methods: the k-shaped classifier and the GMM classifier. The two conventional classifiers have similar procedures with the above DTW-GMM. Therefore, their structures are briefly illustrated in Fig. 5 and Fig. 6, respectively.

2.4 Performance Metrics of Classifier Models

To assess the model recognition performance of the above models, the confusion matrix is a comparative analysis of the model's predictions regarding positive or negative outcomes against the actual class labels of the respective samples. The four key parameters are true positive (TP), false positive (FP), true negative (TN), and false negative (FN) values. Besides, a few indicators, including accuracy (AC), precision (PR), recall (RC), F1 score, and false alarm rate (FAR), are widely utilized to evaluate classifier model efficacy. The formulas of these performance indicators are shown as follows:

$$\text{Accuracy: } AC = \frac{TN + TP}{TN + TP + FN + FP} \quad (10)$$

$$\text{Precision: } PR = \frac{TP}{TP + FP} \quad (11)$$

$$\text{Recall: } RC = \frac{TP}{TP + FN} \quad (12)$$

$$\text{F1 Score: } F1 = \frac{2 \times PR \times RC}{PR + RC} \quad (13)$$

$$\text{False alarm rate: } FAR = \frac{FP}{FP + TN} \quad (14)$$

Larger values of AC, PR, RC, and F1 Score indicate better model performance, but a small FAR value is desirable. These indicators individually evaluate various facets of the classification model, all of them offering a more comprehensive assessment. Specifically, accuracy scrutinizes the overall correctness of predictions; precision emphasizes the accuracy of positive class predictions; recall concentrates on the ability to capture positive instances; the F1 score considers a balance between precision and recall; the false alarm rate evaluates the degree of misclassification for the negative class.

Since the dynamical mode recognition of coupled flickering flame systems is a multi-classification problem, the macro-averaged indicator of multi-class classification can be obtained by the mean value of these performance indicators

$$Macro(AC, PR, RC, F1\ Score, FAR) = \frac{1}{N} \sum_{i=1}^N classes(AC, PR, RC, F1\ Score, FAR)_i \quad (15)$$

where N represents the number of classes, $classes(AC, PR, RC, F1\ Score, FAR)_i$ is the i th $(AC, PR, RC, F1\ Score, FAR)$ value classification.

3. Numerical simulations of flickering flames and data collection

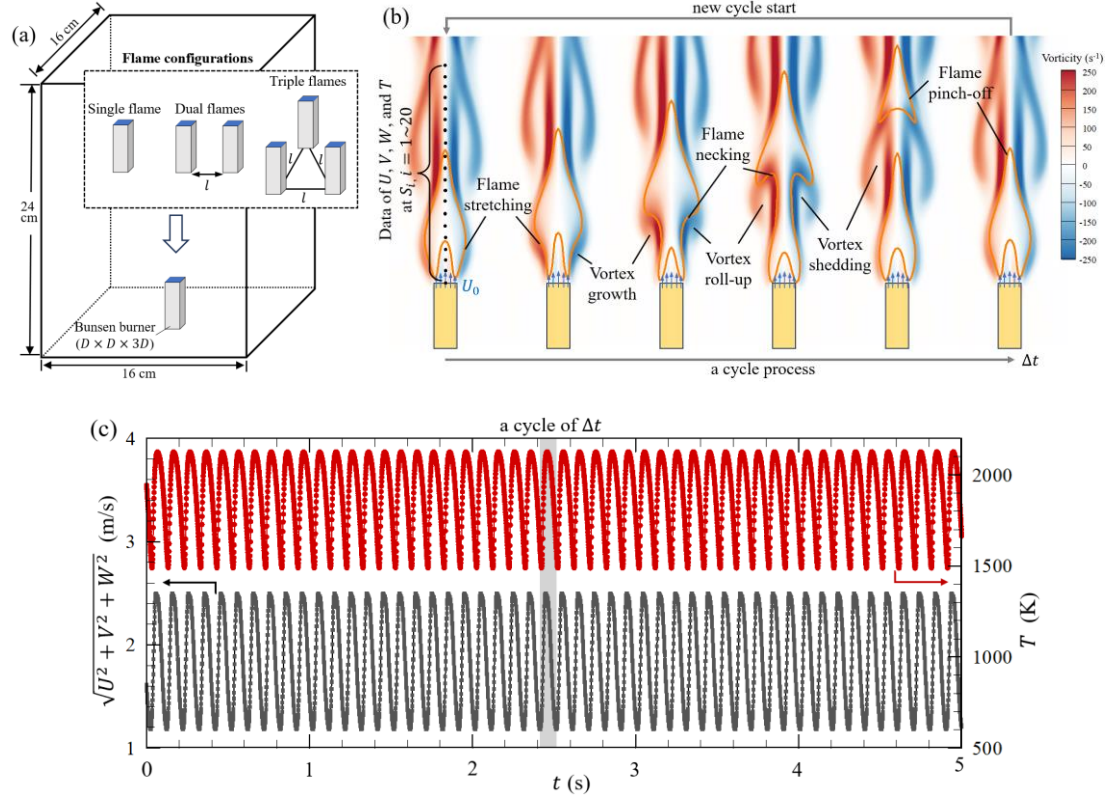


Fig 7. (a) Computational setup of single, dual, and triple flame systems. The Bunsen burner is a cube column of $D \times D \times 3D$, where the top side is set as a fuel inlet of methane with a velocity of U_0 . The dual flame system contains two identical Bunsen burners with a gap distance of l , while three burners are arranged in an equilateral triangle with same distance of l for the triple system. (b) Dynamical behavior of single flickering buoyant diffusion flame: physical features (flame shape and vorticity) during a cycle process of Δt . (c) Time-varying velocity magnitude of $\sqrt{U^2 + V^2 + W^2}$ (m/s) and temperature of T (K) within 5 (s). The data are obtained from the sixth one of 20 sensors arranged equally along the flame center, as shown in Fig. 7(b).

Flame flickering is a prevalent physical phenomenon observed in diffusion flames, premixed flames, and partially premixed flames. Many previous studies [28-31] have found the flicker of diffusion flames is a self-exciting flow oscillation, rather than the results of an externally forced vibration or the alternate flame extinction and re-ignition. The deformation, stretching, or even pinch-off of the flame surface results from the formation and evolution of the toroidal vortices. We utilize this kind of unsteady periodic flame as a prototype of the complex interaction of flame and vortex in many industrial devices, such as gas-stove burners[32], turbomachine rotors[33], can-annular combustors in gas-turbine engines[34, 35]. As shown in Fig. 7(a), the present flame configurations are single, dual, and triple flickering flames, where the Bunsen burner is a cube column of $D \times D \times 3D$ with a fuel inlet of methane with a velocity of U_0 and l is a gap distance between each two identical flames. The detailed descriptions of numerical

schemes, parameters, and validations of present flame simulations can be referred to Supporting Material and the previous studies[36-39].

In a single flickering flame, the deformation, stretching, or even pinch-off of the flame surface results from the formation and evolution of the toroidal vortices. Taking a single flickering flame as an example, the flame flicker is illustrated briefly here. Fig. 7(b) shows the flame shape and the vorticity around the flame during one cycle of $\Delta t \approx 0.1$ s. In physics, the vorticity accumulation inside the toroidal vortex causes the flame deformation; then the rapture of the flame neck can pinch off the flame; finally, the upper portion of the separated flame is convected downstream with the toroidal vortex. Likely, a new circle will start again. Details on the connection between flame flicker and vortex evolution can be referred to [40]. To train and test our proposed models, datasets are obtained from 80 features including 4 variables of velocity components (U , V , and W) and temperature T of 20 sensors, were collected at a sample frequency of 1000 Hz along each flame center for the dimensionality reduction analysis. To further display the periodic oscillation, velocity magnitude and temperature of the sixth sensor during 5s (about 50 cycles) are plotted in Fig. 7(c). The sampling frequency is much higher than the flickering frequency so that small time-scale information of coupled flames can be extracted for our proposed models.

When the gap distance l between each two flames is varied, the dual-flame system and triple-flame system exhibit various dynamical modes, as mentioned in Section 1. Our previous works[36, 37] numerically investigated and theoretically analyzed the dynamical behaviors of dual and triple buoyant diffusion flames. It is key to understand the flickering mechanism of a single buoyant diffusion flame. A brief introduction to coupled flickering flames is given here. From the perspective of vortex dynamics, we attempted to understand the anti-phase and in-phase flickering in a dual-flame system[36], where the interaction between vortex rings of the two flames plays an important role. As shown in Fig.8(a-b), the in-phase mode appears as the three flames flicker synchronously with a negligible phase difference, while the anti-phase mode appears as the flames alternatively flicker with a fixed phase difference of half period. Physically, the transition of the vortical structures from symmetric (in-phase) to staggered (anti-phase) can be interpreted as being similar to the mechanism causing flow transition in the wake of a bluff body and forming the Karman vortex street. Similarly, the four distinct dynamical modes (in-phase, death, rotation, and partially in-phase) of triple flickering buoyant diffusion flames in an equilateral triangle arrangement can be interpreted based on vortex interaction[37]. Specifically, the in-phase mode with a phase difference of 0π in Fig. 8(c) is caused by the periodic shedding of the trefoil vortex formed by the reconnection of three toroidal vortices; the death mode with the flickering suppression (very small oscillation amplitude) in Fig. 8(d) is due to the suppression of vortex shedding at small Reynolds numbers; the rotation mode with a fixed phase difference of $2\pi/3$ in Fig. 8(e) appears as three toroidal vortices alternatively shed off with a constant phase difference; the partially in-phase model (in-phase of two flames but anti-phase to the another one) with 0π and π in Fig. 8(f) is caused by the vorticity reconnection of two toroidal vortices leaving another one shedding off in anti-phase. Therefore, studying coupled flickering flames can be very well to establish a bridge between the vortex dynamics and the nonlinear dynamics of the couple flame system. However, conventional knowledge-based approaches have limits to identifying larger dynamical systems of multiple flames.

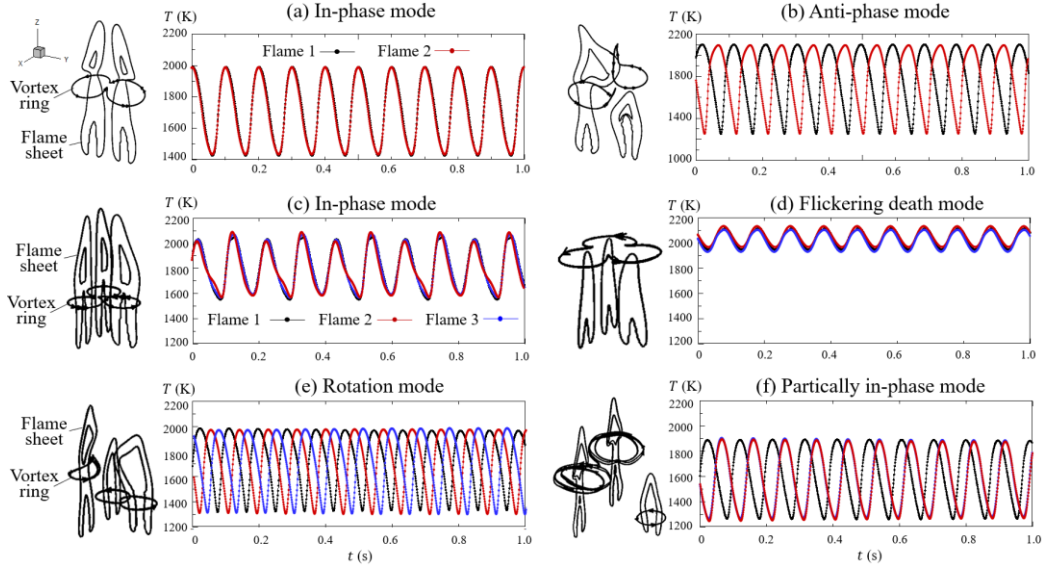


Fig 8. Various dynamical modes induced by vortex interaction and the temperature variation with time of dual- and triple-flame systems: two identical flickering flames[36] in (a) in-phase mode and (b) anti-phase mode; three identical flickering flames[37] in (c) in-phase mode, (d) flickering death mode, (a) rotation mode, and (b) partially in-phase mode.

4. Results and discussion

4.1 Dimensionality reduction of the high-dimensional spatiotemporal flame dataset

As a benchmark comparison of the nonlinear VAE and the linear PCA, Fig. 9(a) and (b) both reveal repeated limit cycles in the continuous phase trajectory in the two-dimensional latent space. However, with the same dimensionality compression ratio, the mean squared error (MSE) error of VAE reconstruction of about 0.2 is smaller than 0.4 of the first two-eigenvalue reconstruction of PCA. In other words, the linear PCA needs at least the first five eigenvalues to be comparable to the nonlinear VAE construction. More details on the MSE error of single, dual, and triple flames are given in Table S2 of the Supporting Material. It should be noted that the complexities of the compared methods are not the same, and the goal of this comparison is to assess how different model architectures affect the quality of the reconstructions. Therefore, the reconstruction performance of VAE becomes increasingly superior to PCA with the increasing complexity of combustion systems.

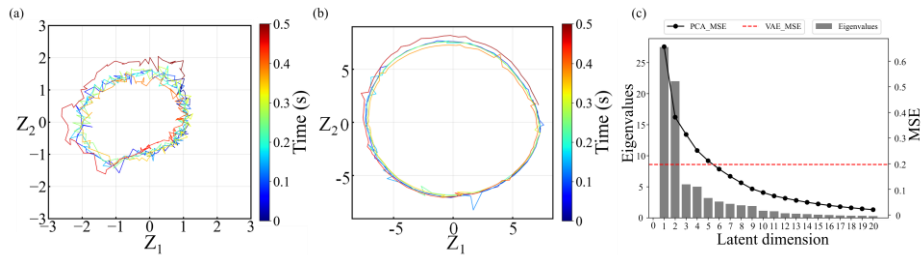


Fig 9. Phase trajectory of the nonlinear oscillation of single buoyant diffusion flame via (a) the latent space of VAE and (b) the first two eigenvalue space of PCA. (c) MSE errors of the present VAE with two latent dimensions and the PCA across various latent dimensions.

Similarly, Fig. 10 compares the dimensionality reduction analysis of VAE and PCA for dual-flame systems and triple-flame systems. The phase distributions in the two-dimensional latent space of VAE

and PCA are depicted, and the different dynamic modes are represented by different colors. The present results show that the shapes of phase trajectories from different scenarios are notably distinct. For the dual-flame system featuring two dynamical modes, both VAE and PCA exhibit distinct separation of phase points representing different modes in the latent space. The trajectory differences representing different modes in latent space are crucial for the deep-learning-based identification of dynamic modes. Otherwise, based on low-dimensional space, labeling flame data as specific modes becomes challenging. However, with the increasing complexity of combustion systems, such as the triple-flame system exhibiting multiple modes, traditional linear methods like PCA often fail to distinctly clarify the various dynamic modes due to their linear constraints. In such cases, PCA may reveal an overlap of phase points representing different modes, blurring the distinction between them. Conversely, VAE demonstrates the ability to maintain a clear separation between modes, owing to its capacity to capture nonlinear relationships. This capability makes VAE a promising approach for tackling complex combustion systems and elucidating the distinct dynamics inherent within them. The distinctive advantage of VAE becomes particularly evident in tasks related to recognizing modes in complex flame systems.

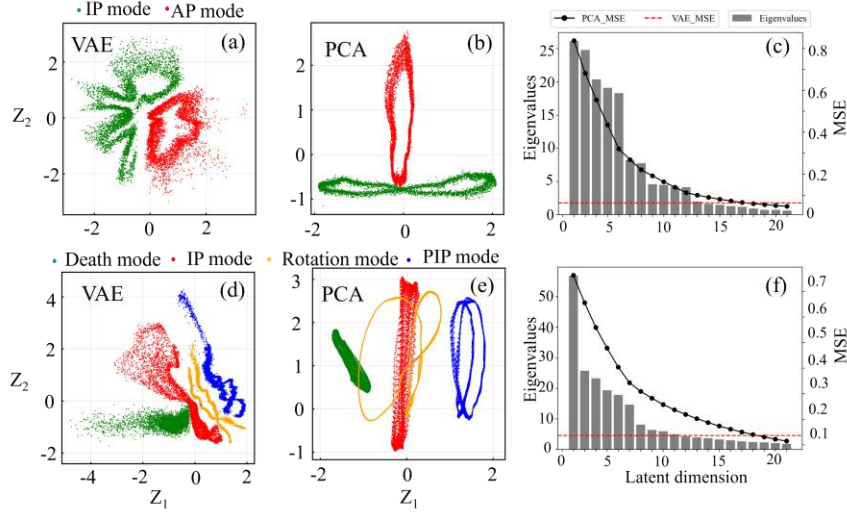


Fig 10. Phase distributions of the multi-flame systems via VAE and PCA: (a-c) dual-flame system and (d-f) triple-flame system. Different colors of phase points represent the different dynamic modes in the combustion systems.

In Conclusion, the dimensional reduction performance of the nonlinear ROM model VAE significantly superior to the linear ROM model PCA in high-dimensional nonlinear combustion systems. Firstly, the linearity makes PCA-based ROM suffer from performance degradation in nonlinear problems, requiring an excessive number of modes compared with nonlinear ROM model VAE for the same reconstruction accuracy. Moreover, while PCA may blur the distinction between different modes by overlapping phase points when projecting data into a lower-dimensional latent space, resulting in poorer performance in subsequent recognition tasks, VAE stands out for its capability to effectively capture nonlinear relationships, thus maintaining a clear separation between modes.

4.2 Wasserstein-distance-based Supervised Classification

In supervised classification, the training data includes 50 cycles with well-labeled data for each mode. To ensure model robustness and effectiveness, 10% of this training dataset is set aside for validation purposes. Additionally, there is a prediction dataset for each mode, consisting of 20 cycles of data. It's noteworthy that all cycles within both the training and prediction datasets share the same time

duration. For each cycle, 1D-WD values are computed in comparison to each benchmark case, which consists of well-labeled data. Specifically, as shown in Fig. 11(a), the prediction dataset for a double flames system with two modes comprises a total of 40 cycles of data. These cycles are individually compared to the In-phase and Anti-phase benchmark datasets to calculate 1D-WD values. A smaller 1D-WD value indicates greater similarity between the two distributions. For instance, the 1D-WD values for the first 20 cycles with the Anti-phase dataset are relatively small, leading to the identification of these cycles as data generated by the Anti-phase mode. Consequently, the subsequent 20 cycles are recognized as data produced by the In-phase mode. This accurate identification process is similarly applicable to the prediction dataset of a triple flames system, as shown in Fig. 11(b), facilitating the recognition of data corresponding to the four modes.

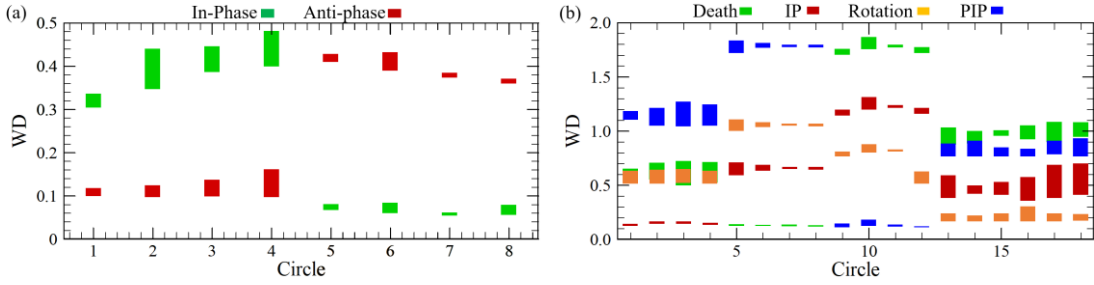


Fig 11. 1D-Wasserstein distance values of the (a) double and (b) triple flame systems. Each circle represents 5 cycles data collected from the combustion systems. Different colors denote the Wasserstein distance values between the prediction data and the benchmark case of the different dynamic modes in the combustion systems.

4.3 GMM-DTWC-based Unsupervised Classification

However, in industrial processes, acquiring a thoroughly labeled dataset is frequently both costly and challenging. Therefore, this study integrates the intrinsic spatial-temporal characteristics of flame data and utilizes the unsupervised machine learning approach GMM-DTW clustering method for unsupervised flame dynamic mode recognition. The training dataset comprises 50 cycles of unlabeled data for each mode, while each mode also boasts a prediction dataset containing 20 cycles. To uphold the model's robustness and effectiveness, 10% of this training dataset is designated for validation purposes.

Fig 12. shows the clustering results of GMM-DTW, GMM, and k -Shape clustering methods in the double flames system and triple flames system. In the clustering results, phase points representing different categories are visually distinguished by using different colors. Where the GMM-DTWC is based on the time trajectories of the phase points by using the DTW algorithm, The GMM clustering method (GMMC) differs from GMM-DTWC by directly utilizing phase point distributions instead of employing DTW to capture periodicity, and the k -Shape clustering method (k -ShapeC) is based on the shape distances of flattened one-dimensional sequences. Whether in a double flames or triple flames system, the clustering results obtained through the proposed GMM-DTWC algorithm closely align with the original point distribution. Conversely, clustering results from the GMMC method and k -ShapeC method exhibit some deviations from the original distribution. In the double flames system with two modes, the GMM-DTWC method accurately identifies each point's mode due to clear separation in the latent space. GMMC and k -ShapeC generally succeed under these conditions. However, in a triple flames system with increased complexity, GMM-DTWC consistently discerns each point's mode accurately, while GMMC and k -ShapeC results deviate significantly from the original distribution.

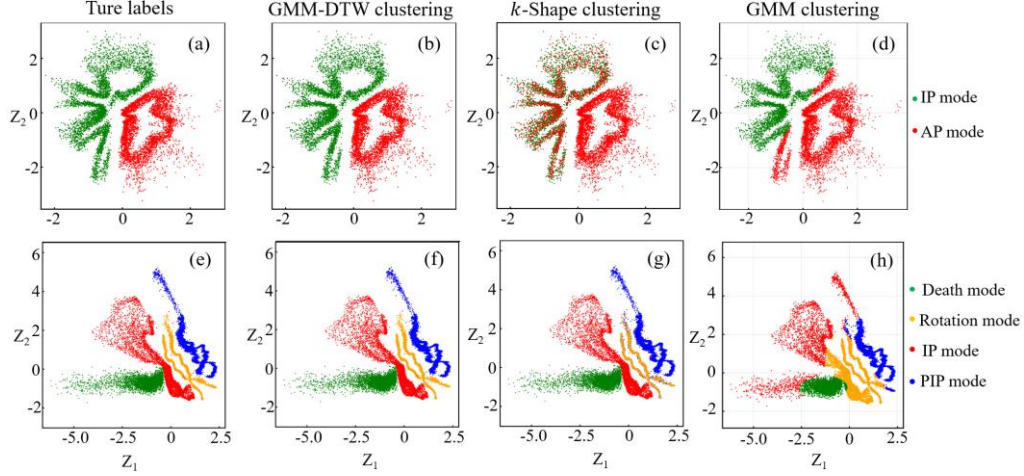


Fig 12. Clustering results of the true labels, GMM-DTW, k -Shape, GMM clustering methods for (a-d) dual-flame and (e-h) triple-flame systems. Different colors of phase points represent the different dynamic modes.

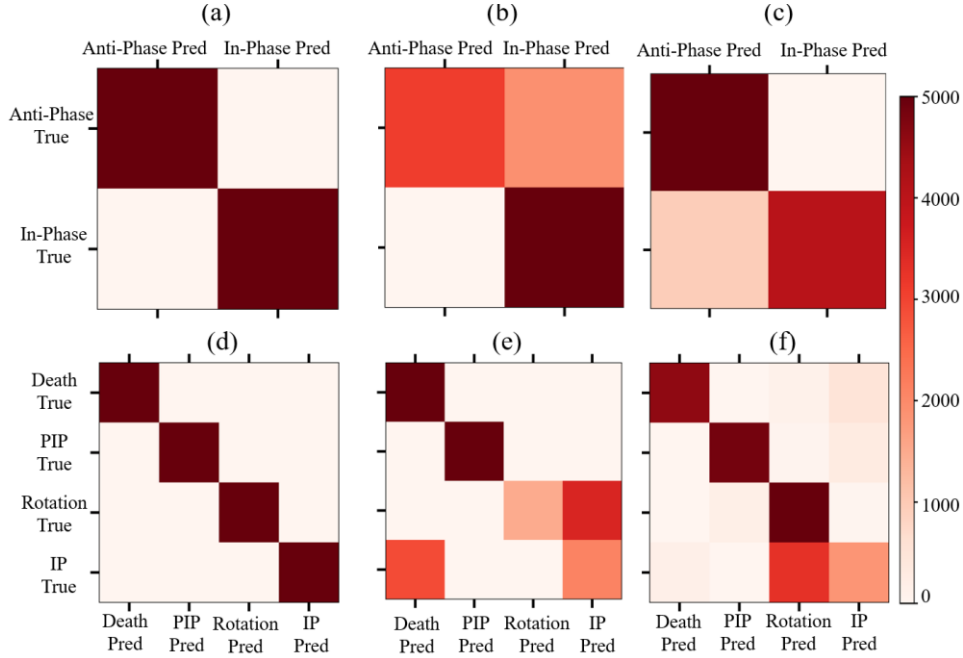


Fig 13. Confusion matrix of the proposed GMM-DTW, k -Shape, GMM clustering methods for (a-c) dual-flame and (d-f) triple-flame systems.

To effectively evaluate the performance of the classifier models, this study utilized a confusion matrix and a set of performance evaluation indicators, including accuracy (AC), precision (PR), recall (RC), F1 score, and false alarm rate (FAR) and their respective macro-average multi-class indicators. We aim to establish an unsupervised effective dynamic mode recognition model for multi-flame systems. Therefore, three unsupervised model recognition models were compared both in the double and triple flames cases. Specifically, Table S3 in the Supporting Material summarizes the recognition performance of the three classification models based on the above indicators. The details of the classification results are analyzed as follows. Fig. 13 shows the dynamic mode recognition confusion matrix using the VAE-GMM-DTWC, VAE-GMMC, and VAE- k -ShapeC methods in the double and triple flame systems. The confusion matrix provides detailed information about the model's predictive performance across different

classes. Based on this information, further calculations can be conducted to derive the above performance indicators, allowing for an in-depth understanding of the model's performance across various categories.

To further quantify the classification model performance and analyze the impact of elaborating the design of each module in the proposed model architecture. Fig. 14 depicts the AC, PR, RC, F1 score, and FAR values in the double flame case and the macro-AC, macro-PR, macro-RC, macro-F1 score, and macro-FAR values in the triple flame case. The overall mean accuracy, precision, recall, and F1 Score values of the VAE-GMM-DTWC method proposed in this study on the two cases are 1, and the FAR is 0. This means the model has an excellent performance among these tasks. Specifically, to verify the effect of considering both the temporal and spatial characteristics of phase points on dynamic mode recognition in complex flame systems, this study conducts a comparative analysis from two perspectives. Firstly, in contrast to the VAE-GMMC method, which incorporates spatial information, the proposed VAE-GMM-DTWC consistently outperforms it in both binary classification (double flames case) and multi-class classification (triple flames case). Positive indicators such as AC, PR, RC, and F1 score (larger values indicating superior model performance) are higher for VAE-GMM-DTWC, while the negative indicator FAR is significantly lower. This highlights the advantage of VAE-GMM-DTWC, emphasizing the importance of considering the temporal characteristics of phase points for accurate dynamic mode recognition in complex flame systems. Additionally, compared to the VAE- k -ShapeC method, which focuses on temporal information, the proposed VAE-GMM-DTWC method demonstrates superior performance in both binary and multi-class classifications. Positive indicators AC, PR, RC, and F1 score are higher for VAE-GMM-DTWC, while the negative indicator FAR is significantly lower. This underscores that the VAE-GMM-DTWC method, accounting for the two-dimensional spatial characteristics of phase points, enhances the accurate recognition of dynamic modes in complex flame systems.

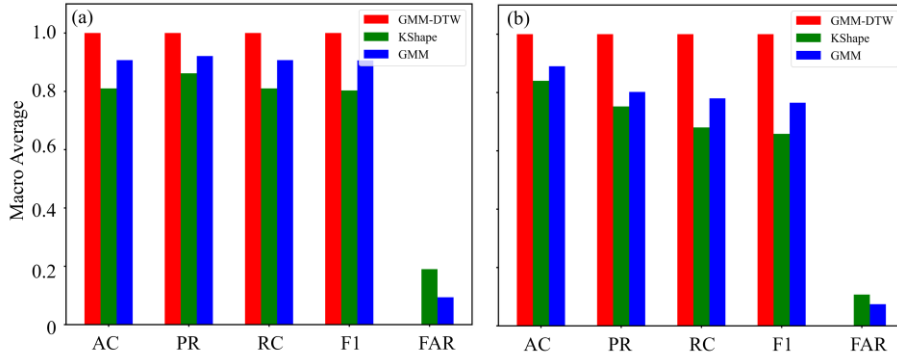


Fig 14. Overall categorized performance of the VAE-GMM-DTWC, VAE-GMMC, and VAE- k Shape methods in (a) dual flames and (b) triple flames.

To further validate the performance of the proposed method in recognizing each subclass in a multi-classification task, this study obtained the AC, PR, RC, F1 score, and FAR values for each category in the case of a triple flame multi-classification. The corresponding values are provided in Table S4 in the Supporting Material. As depicted in Fig. 15, consistent with the overall average performance indicators, the VAE-GMM-DTWC method's positive indicators, including AC, PR, RC, and F1 score, for the four modes, such as Death, PIP, Rotation, and IP, are all 1. These values are significantly higher than those achieved by the GMMC and k -ShapeC methods. Additionally, the negative indicator FAR is 0, notably lower than the GMMC method and k -ShapeC method. This indicates that the GMM method not only

delivers optimal overall classification performance in multi-classification scenarios but also excels in the classification of each subclass.

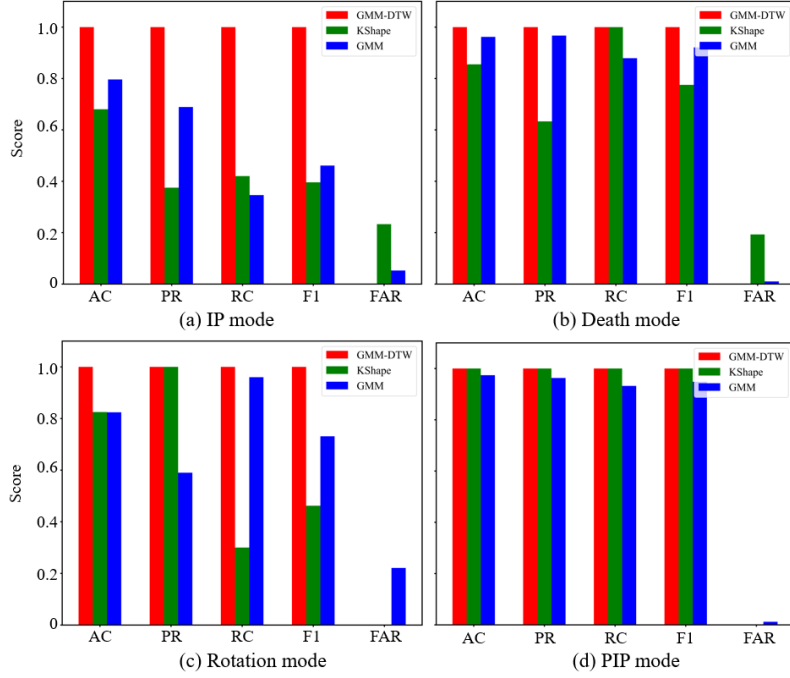


Fig 15. Categorized performance of the proposed VAE-GMM-DTWC method for (a) in-phase, (b) flickering death, (c) rotation, and (d) partially in-phase modes in triple-flame systems.

In summary, as proposed VAE-GMM-DTWC method effectively captures temporal information from dynamic flame systems through the utilization of the time series clustering method GMM-DTWC. The results underscore the robust performance of the proposed method both binary classification (double flames case) and multi-class classification (triple flames case), emphasizing its ability to achieve superior dynamical mode recognition outcomes, characterized by both high accuracy and minimal false alarm rates. This indicates the potential of the proposed approach to address the challenges in complex coupled flame oscillators systems.

5. Conclusions

Nonlinear dynamics of coupled oscillators is a long-lasting problem in the science of complex systems. The work presented in this study takes a baby step toward the objective by studying the collective dynamics behaviors of coupled flame oscillators made of unsteady laminar flickering diffusion flames. Different from the conventional approaches of nonlinear dynamics and complex systems theory, we adopted machine learning-based approaches to provide new perspectives to recognize and interpret various dynamical patterns of the coupled flame oscillators.

Specifically, a VAE-WDC supervised classification model and a VAE-GMM-DTWC unsupervised classification model for binary classification and multiclassification identification of coupled flame oscillator systems are established in this work. The data are collected from the numerical simulations of diverse dynamical modes in single-, double-, and triple-flame systems. These simulations involve solving for the buoyancy-driven flickering flame using an unsteady, three-dimensional, low-Mach, and variable-density chemically reacting flow with a simplified chemical reaction mechanism. Each dataset comprises a time series with 80 features in a single flame, where four variables (U , V , W , and T) were sampled at 1000 Hz for 5 seconds (approximately 50 flickering periods) along the central axis of each flame.

Based on supervised and unsupervised methods of deep learning, we developed a robust and comprehensive framework for dynamical mode recognition of coupled flame oscillators, which has the potential for larger combustion systems made of real turbulent flames. The established nonlinear dimensional reduction VAE model is effective in projecting the high-dimensional raw data from multi-flame systems onto a 2-dimensional phase space defined by two latent variables, providing a data-driven-based feature extraction approach compared to expert knowledge-based methods. It holds the potential for overcoming the limitations of feature extraction through expert knowledge and for applications in high-complexity nonlinear dynamic systems.

Additionally, based on the dimensionality reduction of deep learning, we provided new ways of classifying these reduced spatiotemporal data of the coupled flame oscillators. For datasets with sufficient labels, we consider the distribution of flame data with sufficient labels in the phase space as the benchmark dataset, then implement supervised mode recognition using the Wasserstein distance as a quantitative measure of proximity between two probability distributions in latent space. Addressing unlabeled time series, we combine dynamic time warping (DTW) and an unsupervised Gaussian mixture model (GMM) to achieve effective dynamic flame mode recognition based on phase point trajectories. Both supervised and unsupervised mode recognition approaches yield favorable classification results. In conclusion, the present work demonstrates the first successful attempt at providing a robust and comprehensive framework for mode recognition in coupled flickering flames. The framework has the potential to deal with more complex systems consisting of more flame oscillators.

Declaration of competing interest

The authors declare that they have no conflict of interest.

Acknowledgments

This work is supported by the National Natural Science Foundation of China (No. 52176134) and partially by the APRC-CityU New Research Initiatives/Infrastructure Support from Central of City University of Hong Kong (No. 9610601).

Supplementary material

Supplementary material includes the details of the present VAE formulation, the numerical simulations, the reconstruction loss of training and validating VAE, and the evaluation results for single, double-, and triple-flame systems.

Author Contributions

Weiming Xu: Conceptualization (equal); Data curation (equal); Formal analysis (equal); Investigation (equal); Methodology (lead); Visualization (equal); Writing – original draft (equal). **Tao Yang:** Conceptualization (equal); Data curation (equal); Formal analysis (equal); Investigation (equal); Simulation (lead); Visualization (equal); Writing – original draft (equal). **Peng Zhang:** Conceptualization (equal); Investigation (equal); Supervision (lead); Writing – review and editing (lead).

References

- [1] K. McManus, T. Poinso, S.M. Candel, A review of active control of combustion instabilities, *Progress in energy and combustion science*, 19 (1993) 1-29.
- [2] D. Chamberlin, A. Rose, The flicker of luminous flames, *Industrial & Engineering Chemistry*, 20 (1928) 1013-1016.

- [3] D. Moreno-Boza, W. Coenen, J. Carpio, A.L. Sánchez, F.A. Williams, On the critical conditions for pool-fire puffing, *Combust. Flame*, 192 (2018) 426-438.
- [4] D. Durox, T. Yuan, F. Baillot, J. Most, Premixed and diffusion flames in a centrifuge, *Combust. Flame*, 102 (1995) 501-511.
- [5] N. Fujisawa, T. Okuda, Effects of co-flow and equivalence ratio on flickering in partially premixed flame, *International Journal of Heat and Mass Transfer*, 121 (2018) 1089-1098.
- [6] H. Kitahata, J. Taguchi, M. Nagayama, T. Sakurai, Y. Ikura, A. Osa, Y. Sumino, M. Tanaka, E. Yokoyama, H. Miike, Oscillation and synchronization in the combustion of candles, *The Journal of Physical Chemistry A*, 113 (2009) 8164-8168.
- [7] K. Okamoto, A. Kijima, Y. Umeno, H. Shima, Synchronization in flickering of three-coupled candle flames, *Sci. Rep.*, 6 (2016) 1-10.
- [8] K. Manoj, S.A. Pawar, R. Sujith, Experimental investigation on the susceptibility of minimal networks to a change in topology and number of oscillators, *Physical Review E*, 103 (2021) 022207.
- [9] V. Nair, R. Sujith, A reduced-order model for the onset of combustion instability: physical mechanisms for intermittency and precursors, *Proceedings of the combustion institute*, 35 (2015) 3193-3200.
- [10] R. Swischuk, B. Kramer, C. Huang, K. Willcox, Learning physics-based reduced-order models for a single-injector combustion process, *AIAA Journal*, 58 (2020) 2658-2672.
- [11] T. Hummel, K. Hammer, P. Romero, B. Schuermans, T. Sattelmayer, Low-order modeling of nonlinear high-frequency transversal thermoacoustic oscillations in gas turbine combustors, *Journal of Engineering for Gas Turbines and Power*, 139 (2017) 071503.
- [12] A. Maćkiewicz, W. Ratajczak, Principal components analysis (PCA), *Computers & Geosciences*, 19 (1993) 303-342.
- [13] G. Berkooz, P. Holmes, J.L. Lumley, The proper orthogonal decomposition in the analysis of turbulent flows, *Annu. Rev. Fluid Mech.*, 25 (1993) 539-575.
- [14] J.P. Cunningham, Z. Ghahramani, Linear dimensionality reduction: Survey, insights, and generalizations, *The Journal of Machine Learning Research*, 16 (2015) 2859-2900.
- [15] M. Ihme, W.T. Chung, A.A. Mishra, Combustion machine learning: Principles, progress and prospects, *Prog. Energy Combust. Sci.*, 91 (2022) 101010.
- [16] F. Arai, K. Iemura, M. Saito, M. Tanabe, Study on Nonlinear Dynamics Using the State Space of Combustion Oscillation in a Rocket Combustor, *Trans.Japan.Soc.Aero.Space.Sci.*, 66 (2023) 156-163.
- [17] K. Iemura, M. Saito, Y. Suganuma, M. Kikuchi, Y. Inatomi, H. Nomura, M. Tanabe, Analysis of spatial-temporal dynamics of cool flame oscillation phenomenon occurred around a fuel droplet array by using variational auto-encoder, *Proceedings of the Combustion Institute*, 39 (2023) 2523-2532.
- [18] W. Xu, T. Yang, P. Zhang, Dimensionality Reduction and Dynamical Mode Recognition of Circular Arrays of Flame Oscillators Using Deep Neural Network, *arXiv preprint arXiv:2312.02462*, (2023).
- [19] X. Liu, C. Yao, J. Chen, E. Song, Modeling of 0-D heat release rate of heavy-duty diesel engine based on classification algorithm, *International Journal of Engine Research*, 24 (2022) 2437-2450.
- [20] Z. Wang, C. Song, T. Chen, Deep learning based monitoring of furnace combustion state and measurement of heat release rate, *Energy*, 131 (2017) 106-112.
- [21] F. Liu, X. Li, X. Hu, S. Li, Y. Liu, Q. Shi, in: *The proceedings of the 16th Annual Conference of China Electrotechnical Society: Volume I*, Springer, 2022, pp. 701-707.

- [22] S. Barwey, V. Raman, Data-driven reduction and decomposition with time-axis clustering, *Proceedings of the Royal Society A: Mathematical, Physical and Engineering Sciences*, 479 (2023) 20220776.
- [23] R. Mishra, S. Mayilvahanan, D. Jarrahbashi, Hybrid Unsupervised Cluster-wise Regression Approach for Representing the Flamelet Tables, *Energy & Fuels*, 37 (2023) 3056-3070.
- [24] L. Castellanos, R. Da Silva Machado De Freitas, A. Parente, F. Contino, A time-lag autoencoder reduced-order model to predict combustion chemical kinetics, (2023).
- [25] V.M. Panaretos, Y. Zemel, Statistical aspects of Wasserstein distances, *Annual review of statistics and its application*, 6 (2019) 405-431.
- [26] Y. Chi, T. Yang, P. Zhang, Dynamical mode recognition of triple flickering buoyant diffusion flames in Wasserstein space, *Combust. Flame*, 248 (2023) 112526.
- [27] L.V. Kantorovich, On the translocation of masses, *Journal of mathematical sciences*, 133 (2006) 1381-1382.
- [28] J. Buckmaster, N. Peters, The infinite candle and its stability—a paradigm for flickering diffusion flames, *Symposium (International) on Combustion*, 21 (1988) 1829-1836.
- [29] X. Jiang, K. Luo, Combustion-induced buoyancy effects of an axisymmetric reactive plume, *Proc. Combust. Inst.*, 28 (2000) 1989-1995.
- [30] M.P. Juniper, L.K. Li, J.W. Nichols, Forcing of self-excited round jet diffusion flames, *Proc. Combust. Inst.*, 32 (2009) 1191-1198.
- [31] D. Moreno-Boza, W. Coenen, A. Sevilla, J. Carpio, A. Sánchez, A. Liñán, Diffusion-flame flickering as a hydrodynamic global mode, *J. Fluid Mech.*, 798 (2016) 997-1014.
- [32] S.-S. Hou, C.-Y. Lee, T.-H. Lin, Efficiency and emissions of a new domestic gas burner with a swirling flame, *Energy Conversion and Management*, 48 (2007) 1401-1410.
- [33] N. Peake, A.B. Parry, Modern challenges facing turbomachinery aeroacoustics, *Annu. Rev. Fluid Mech.*, 44 (2012) 227-248.
- [34] Y. Xia, C. Linghu, Y. Zheng, C. Ye, C. Ma, H. Ge, G. Wang, Experimental investigation of the flame front propagation characteristic during light-round ignition in an annular combustor, *Flow, Turbulence and Combustion*, 103 (2019) 247-269.
- [35] K. Moon, Y. Choi, K.T. Kim, Experimental investigation of lean-premixed hydrogen combustion instabilities in a can-annular combustion system, *Combust. Flame*, 235 (2022) 111697.
- [36] T. Yang, X. Xia, P. Zhang, Vortex-dynamical interpretation of anti-phase and in-phase flickering of dual buoyant diffusion flames, *Physical review fluids*, 4 (2019) 053202.
- [37] T. Yang, Y. Chi, P. Zhang, Vortex interaction in triple flickering buoyant diffusion flames, *Proceedings of the Combustion Institute*, 39 (2023) 1893-1903.
- [38] T. Yang, P. Zhang, Faster flicker of buoyant diffusion flames by weakly rotatory flows, *Theoretical and Computational Fluid Dynamics*, (2023) 1-18.
- [39] T. Yang, Y. Ma, P. Zhang, Computational Investigation on Collective Dynamical Behaviors of Flickering Laminar Buoyant Diffusion Flames in Circular Arrays, *arXiv preprint arXiv:2312.02018*, (2023).
- [40] X. Xia, P. Zhang, A vortex-dynamical scaling theory for flickering buoyant diffusion flames, *J. Fluid Mech.*, 855 (2018) 1156-1169.